necessary to produce reliable results.

The rotamer populations of the $-CH_2OH$ side chain were calculated according to equations 4.11-4.13 of Davies.[36] The results are as follows: 45% gauche$^+$, 36% trans, and 19% gauche$^-$. As usual, the gauche$^+$ conformation predominates, but its contribution is not as large as in purine nucleosides. These results can be attributed to electrostatic repulsion between N(2) and O(5'). The distance between these two atoms would be very short (<3.0 Å) if the furanose ring was in the C(2') endo/C(3') exo and the side chain in the gauche$^+$ conformation. Consequently, the gauche$^+$ rotamer can occur only when the ring pucker is C(3') endo/C(4') exo.

**Acknowledgments.** Apart from MULTAN78,[18] all crystallographic computations were carried out with programs written by Ahmed et al.[37] Figures 1 and 4 were drawn with the ORTEP program of Johnson.[38] Haasnoot's program CAGPLUS, which relates vicinal coupling constants to torsion angles between protons,[34] was used to determine the conformation of the diazepine ring.

**Registry No. 2**, 98720-84-4.

**Supplementary Material Available:** Tables of anisotropic temperature parameters and a list of observed and calculated structure amplitudes (8 pages). Ordering information is given on any current masthead page.

(36) Davies, D. B. *Progr. Nucl. Magn. Reson. Spectrosc.* **1978**, 135-225.

(37) Ahmed, F. R.; Hall, S. R.; Pippy, M. E.; Huber, C. P. *J. Appl. Crystallogr.* **1973**, *6*, 309-346.

(38) Johnson, C. K. ORTEP II Report ORNL-5138, Oak Ridge National Laboratory, Oak Ridge, TN, 1976.

# βI- and βII-Turn Conformations in Model Dipeptides with the Pro-Xaa Sequences

**A. Aubry,[1a] M. T. Cung,[1b] and M. Marraud*[1b]**

*Contribution from The Laboratory of Mineralogy and Crystallography, University I of Nancy, CNRS-UA-04-809, 54506 Vandoeuvre-les-Nancy Cêdex, France, and The Laboratory of Macromolecular Physical Chemistry, ENSIC-INPL, CNRS-UA-04-494, 54042 Nancy Cêdex, France.* *Received May 15, 1985*

**Abstract:** Model dipeptides *t*-BuCO-L-Pro-Xaa-NHMe (Xaa = L- or D-Leu, Val, Cys, Met, Phe, and Tyr) with an aliphatic, aromatic, or weakly polar Xaa side chain have been investigated in solution by IR and $^1H$ NMR spectroscopies and in the solid state by X-ray diffraction. The heterochiral dipeptides L-Pro-D-Xaa are found to accommodate the same βII-turn conformation in both states. The homochiral dipeptides L-Pro-L-Xaa experience more conformational freedom since the β-turn conformation is shown to be of the βI type in solution and of the βII type in the crystal. This conformational change probably arises from the molecular packing forces and essentially from an intermolecular hydrogen bond between the Xaa NH and C'O groups of two neighboring molecules. This shows that the βII-turn conformation is a stable disposition of a LL-dipeptide sequence provided there is some energy compensation through an intermolecular interaction in oligopeptides or a long-range interaction in larger peptides.

β-Folded regions or β-turns are conformational units of primary importance for the three-dimensional structure of peptides and proteins.[2,3] Four consecutive amino acid residues indexed from $i$ to $(i + 3)$ are arranged in such a way that the peptide chain is folded back on itself, giving rise to the globular character of the proteins.

Ten types of peptide chain reversals have been found in crystallized proteins.[4] Three of them containing an intramolecular hydrogen bond of the $(i + 3) \rightarrow i$ type are denoted βI-, βII-, and βVI-turns, and they differ by the rotational angles associated with the $(i + 1)$ and $(i + 2)$ residues.[5] The βVI-turn is also characterized by the cis disposition of the amide bond between the $(i + 1)$ and $(i + 2)$ residues, and it exclusively concerns L-Xaa-L-Pro[3] and L-Xaa-Me-L-Yaa sequences.[6,7]

The biological importance[2] and the frequent occurrence of β-turns in proteins[3] (32% residues are involved in a β-turn) and peptides[8] have justified the considerable amount of statistical, theoretical, and experimental work dealing with this particular conformational unit.[2] After the first experimental characterization of a β-turn in the crystal structures of cyclohexaglycine[9] and ferrichrome A,[10] Venkatachalam performed pioneering conformational calculations in which atoms were taken as hard spheres.[11] He concluded that different stereochemical sequences defined by the $(i + 1)$ and $(i + 2)$ residues should correspond to different β-turns. Homochiral LL sequences and heterochiral LD sequences should prefer the so-called βI and βII dispositions, respectively. The achiral glycyl residue G was predicted to equally accomodate both the L and D dispositions. The enantiomeric sequences should of course favor the symmetrical dispositions denoted as βI'- (DD) and βII'-turns (DL). These conclusions were then corroborated by more sophisticated calculations using empirical,[12-17] semi-

(1) (a) University of Nancy I. (b) ENSIC-INPL.

(2) (a) Smith, J. A.; Pease, L. G. *CRC Crit. Rev. Biochem.* **1980**, *8*, 315-399. (b) Rose, G. D.; Glerasch, L. M.; Smith, J. A. *Adv. Protein Chem.* **1985**, *37*, 1-109.

(3) Chou, P. Y.; Fasman, G. D. *J. Mol. Biol.* **1977**, *115*, 135-175.

(4) Lewis, P. N.; Momany, F. A.; Scheraga, H. A. *Biochim. Biophys. Acta* **1973**, *303*, 211-229.

(5) The idealized torsional angles for β-turns are the following: type I, $\Phi_{i+1} = -60°$, $\psi_{i+1} = -30°$, $\Phi_{i+2} = -90°$, $\psi_{i+2} = 0°$; type II, $\Phi_{i+1} = -60°$, $\psi_{i+1} = 130°$, $\Phi_{i+2} = 90°$, $\psi_{i+2} = 0°$; type VI, $\Phi_{i+1} = -60°$, $\psi_{i+1} = 130°$, $\omega_{i+1} = 0°$, $\Phi_{i+2} = -120°$, $\psi_{i+2} = 60°$. The designation of different βI- and βIII-bend types seems to be rather artificial and does not apply to those simple model dipeptides.

(6) Iitaka, Y.; Nakamura, H.; Takada, K.; Takita, T. *Acta Crystallogr., Sect. B* **1974**, *30*, 2817-2825.

(7) Vitoux, B.; Aubry, A.; Cung, M. T.; Boussard, G.; Marraud, M. *Int. J. Peptide Protein Res.* **1981**, *17*, 469-479.

(8) Karle, I. L. In "The Peptides; Analysis, Synthesis, Biology"; Gross, E., Meienhofer, J., Eds.; Academic Press: New York, 1981; Vol. IV, pp 1-54.

(9) Karle I. L.; Karle, J. *Acta Crystallogr.* **1963**, *16*, 969-975.

(10) Zalkin, A.; Forrester, J. D.; Templeton, D. H. *J. Am. Chem. Soc.* **1966**, *88*, 1810-1814.

(11) Venkatachalam, C. M. *Biopolymers* **1968**, *6*, 1425-1436.

0002-7863/85/1507-7640$01.50/0 

Table I. Unit Cell Dimensions and Other Crystal Data

| | i-PrCO-L-Pro-L-Ala-NH-i-Pr[a] | t-BuCO-L-Pro-L-Leu-NHMe | t-BuCO-L-Pro-L-Cys(Me)-NHMe | t-BuCO-L-Pro-L-Phe-NHMe | t-BuCO-L-Pro-L-Tyr-NHMe | t-BuCO-L-Pro-D-Tyr-NHMe | i-PrCO-L-Pro-D-Ala-NH-i-Pr[a] |
|---|---|---|---|---|---|---|---|
| space group | $P2_1$ | $P2_1$ | $P2_1$ | $P2_12_12_1$ | $P1$ | $P2_1$ | $P2_1$ |
| $Z$ | 2 | 2 | 2 | 4 | 1 | 2 | 2 |
| $a$, Å | 9.95 (2) | 9.883 (1) | 9.642 (1) | 20.951 (4) | 5.715 (1) | 5.228 (1) | 10.46 (2) |
| $b$, Å | 9.74 (2) | 9.518 (1) | 9.842 (1) | 17.331 (4) | 7.736 (1) | 15.043 (2) | 9.11 (2) |
| $c$, Å | 9.68 (2) | 10.678 (2) | 9.646 (1) | 5.440 (1) | 11.450 (2) | 11.540 (1) | 9.70 (2) |
| $\alpha$, deg | | | | | 86.53 (2) | | |
| $\beta$, deg | 109.4 (1) | 100.17 (1) | 99.76 (1) | | 82.39 (2) | 96.84 (1) | 108.2 (1) |
| $\gamma$, deg | | | | | 84.96 (2) | | |
| $d$(calcd) | 1.12 | 1.09 | 1.21 | 1.21 | 1.24 | 1.21 | 1.04 |
| independent reflections | | 2003 | 1816 | 2189 | 1887 | 2020 | |
| unique reflections | | 1808[b] | 1312[c] | 1589[c] | 1810[b] | 1892[b] | |
| final $R$ | | 0.048 | 0.052 | 0.058 | 0.033 | 0.045 | |
| final $R_w$ | | 0.058 | 0.060 | 0.054 | 0.031 | 0.051 | |
| $1/w$ | | $\sigma^2(F) + 0.0057F^2$ | $\sigma^2(F) + 0.0554F^2$ | $\sigma^2(F) + 0.0219F^2$ | $\sigma^2(F)$ | $\sigma^2(F) + 0.0069F^2$ | |

[a] From ref 20. [b] $I > 2\sigma(I)$. [c] $I > 3\sigma(I)$.

empirical,[18] and ab initio methods.[19]

Experimental findings essentially confirm the above-mentioned calculations, especially the X-ray structures of peptides[8] and proteins.[3] However, some discrepancies have been pointed out by X-ray crystallography: a βII-folded L-Pro-L-Ala sequence in i-PrCO-L-Pro-L-Ala-NH-i-Pr;[20] a βI′-folded L-Leu-Gly sequence in cyclo(Gly-L-Leu-Gly)$_2$, $2H_2O$;[21] two βI′-folded Aib-L-Ala and L-Ala-Aib sequences in Z(Cl)-L-Pro-Aib-L-Ala-Aib-L-Ala-OMe;[22] and, a βII′-folded L-Phe-L-Ala sequence in cyclo(L-Pro-L-Val-L-Phe-L-Phe-L-Ala-Gly).[23] Moreover, 10% of the β-folded LL sequences in crystallized proteins are of the βII type.[3]

For several years, we have been engaged in extensive investigations of model dipeptides RCO-Xaa-Yaa-NHR′ which are the most simple molecules compatible with β-folding.[24,25] We have previously reported that the homochiral dipeptide i-PrCO-L-Pro-L-Ala-NH-i-Pr experiences a conformational transition (βI to βII-folding mode) when changing from the solute[24] to the crystalline state.[20] Under the same conditions, the heterochiral dipeptide i-PrCO-L-Pro-D-Ala-NH-i-Pr accommodates the same βII-folding mode.[20,24]

Investigations have been focused on the t-BuCO-L-Pro-Xaa-NHMe dipeptides in which Xaa is a L or D residue. The present paper concerns the dipeptides with Xaa having an apolar (Leu, Val), weakly polar (Cys, Met), or aromatic (Phe, Tyr) side chains. Experiments have been carried out in solution by IR and $^1$H NMR spectroscopies. The X-ray crystal structures of five dipeptides which grew good single crystals (Xaa = L-Leu, L-Cys(Me), L-Phe, L-Tyr, and D-Tyr) confirm that the above conformational transition is a general property of the homochiral L-Pro-L-Xaa dipeptides.

## Experimental Section

**Synthesis.** The model dipeptides t-BuCO-L-Pro-Xaa-NHMe have been obtained by classical procedures using *tert*-butyloxycarbonyl (BOC) as an intermediary N-protection and dicyclohexylcarbodiimide as the coupling reagent. The pivaloyl group (t-BuCO) was introduced on proline by action of the pivaloyl chloride. It was preferred to the more classical BOC group because of a twofold advantage: (i) absence of the cis conformer for the t-BuCO-Pro amide bond[26] and (ii) more peptide-like character with a higher basicity of the carbonyl group giving higher β-folding ratios.

Three types of Cys-containing dipeptides have been prepared with free SH cysteine (Xaa = L-Cys), cystine (Xaa = L-cys), and S-methylcysteine (Xaa = L- or D-Cys(Me)). The free SH derivative was obtained from *S-tert*-butyl-L-cysteine and S-deprotection by tributylphosphine.

In the following text, the model dipeptides are abbreviated by their L-Pro-Xaa sequence.

**X-ray Diffraction.** Five dipeptides with Xaa = L-Leu, L-Phe, L-Cys(Me), L-Tyr, and D-Tyr have grown single crystals by slow evaporation of an ethyl acetate solution. X-ray data were collected at room temperature on an Enraf Nonius CAD 4 automatic diffractometer, with a graphite monochromator and the Cu Kα radiation (λ = 1.540 51 Å), in the $\theta$–$2\theta$ scanning mode ($\theta \leq 70°$). Intensity data were corrected for decay when three standard reflections decreased by more than 5% and corrected for Lorentz and polarization effects. Due to the small size (<0.3 mm) of the single crystals, the absorption was neglected. Cell dimensions obtained by refinement from a set of 25 high-angle reflections are indicated in Table I together with other experimental parameters.

The structures were solved by direct methods by using the computer program MULTAN-80[27] and refined using a full matrix least-square procedure.[28] Atom-scattering factors used were those listed in the "International Tables for X-ray Crystallography".[29] E-maps revealed all the non-hydrogen atoms and two equally occupied positions called A and B for the $C^\gamma$ atom in L-Pro-L-Cys(Me). Most hydrogen atoms were located in difference maps. Refined parameters were calculated by using anisotropic temperature factors for the non-hydrogen atoms and fixed isotropic thermal factors for the hydrogen atoms. The function minimized by the least squares was

$$\sum w|k|F_o| - |F_c||^2$$

where the weights $w$ are given in Table I together with the final factors

$$R = \sum k||F_o| - |F_c||/\sum k|F_o|$$

and

$$R_w = \sum w|k|F_o| - |F_c||/\sum wk|F_o|$$

For a reliable comparison of the inter- and intramolecular hydrogen bond dimensions, and following Taylor and Kennard,[30] OH and NH hydrogen atoms were replaced at 1.03 Å from O and N in the direction

(12) Chandrasekaran, R.; Lakshminarayanan, A. V.; Pandya, U. V.; Ramachandran, G. N. *Biochim. Biophys. Acta* **1973**, *303*, 14–27.
(13) Nishikawa, K.; Momany, F. A.; Scheraga, H. A. *Macromolecules* **1974**, *7*, 797–806.
(14) Momany, F. A.; McGuire, R. F.; Burgess, A. W.; Scheraga, H. A. *J. Phys. Chem.* **1975**, *79*, 2361–2381.
(15) Zimmerman, S. S.; Scheraga, H. A. *Biopolymers* **1977**, *16*, 811–843.
(16) Popov, E. M. *Int. J. Quantum Chem.* **1979**, *16*, 707–737.
(17) Chuman, H.; Momany, F. A.; Schäfer, L. *Int. J. Peptide Protein Res.* **1984**, *24*, 233–248.
(18) Maigret, B.; Pullman, B. *Theor. Chim. Acta* **1974**, *35*, 113–128.
(19) Peters, D.; Peters, J. *J. Mol. Struct.* **1980**, *62*, 229–247.
(20) Aubry, A.; Protas, J.; Boussard, G.; Marraud, M. *Acta Crystallogr., Sect. B* **1977**, *33*, 2399–2406.
(21) Brown, J. N.; Rosen, L. S. *Cryst. Struct. Commun.* **1981**, *10*, 591–595.
(22) Cameron, T. S.; Hanson, A. W.; Taylor, A. *Cryst. Struct. Commun.* **1982**, *11*, 321–330.
(23) Chiang, C. C.; Karle, I. L.; Wieland, T. *Int. J. Peptide Protein Res.* **1982**, *20*, 414–420.
(24) Boussard, G.; Marraud, M.; Aubry, A. *Biopolymers* **1979**, *18*, 1297–1331.
(25) Boussard, G.; Marraud, M. *J. Am. Chem. Soc.* **1985**, *107*, 1825–1828.
(26) Nishihara, H.; Nishihara, K.; Uefuji, T.; Sakota, N. *Bull. Chem. Soc. Jpn.* **1975**, *48*, 553–555.
(27) Main, P.; Fiske, S. J.; Hall, S. E.; Lessinger, L.; Germain, G.; Declerq, J. P.; Woolfson, M. M. "MULTAN 80"; Universities of York: England and Louvain, Belgium; 1980.
(28) Sheldrick, G. M. "Programs for Crystal Structure Determination"; University of Cambridge: England, 1976.
(29) "International Tables for X-Ray Crystallography"; Kynoch Press: Birmingham, 1974; Vol. IV.
(30) Taylor, R.; Kennard, O. *Acta Crystallogr., Sect. B.* **1983**, *39*, 133–138.

Table II. Molecular Conformations[a]

| | L-Pro-L-Ala[b] | L-Pro-L-Leu | L-Pro-L-Cys(Me) | L-Pro-L-Phe | L-Pro-L-Tyr | L-Pro-D-Tyr | L-Pro-D-Ala[b] |
|---|---|---|---|---|---|---|---|
| $\phi_1$ | −59 | −61.6 | −60.6 | −63.5 | −55.6 | −58.8 | −62 |
| $\psi_1$ | 136 | 134.6 | 132.0 | 138.7 | 134.9 | 137.4 | 137 |
| $\phi_2$ | 66 | 60.9 | 62.4 | 62.0 | 64.4 | 72.9 | 96 |
| $\psi_2$ | 14 | 23.7 | 17.0 | 22.8 | 16.3 | 9.0 | 3 |
| $\omega_0$ | 177 | 178.5 | 174.6 | 173.8 | 173.8 | 173.4 | −178 |
| $\omega_1$ | 180 | 178.3 | −178.0 | −178.8 | 178.2 | −176.3 | 180 |
| $\omega_2$ | 179 | −179.4 | −173.5 | −178.9 | 178.0 | 179.9 | 178 |
| $\chi_1^1$ | | 19.8 | 24.2[c] | 29.8 | −28.4 | −23.3 | |
| | | | −19.3[d] | | | | |
| $\chi_1^2$ | | −31.5 | −37.6[c] | −37.8 | 39.8 | 36.6 | |
| | | | 32.7[d] | | | | |
| $\chi_1^3$ | | 30.4 | 35.9[c] | 30.6 | −35.6 | −35.6 | |
| | | | −31.7[d] | | | | |
| $\chi_1^4$ | | −17.6 | −20.4[c] | −12.3 | 18.4 | 22.1 | |
| | | | 20.9[d] | | | | |
| $\chi_1^5$ | | −1.6 | −1.3 | −11.2 | 6.2 | 0.5 | |
| $\chi_2^1$ | | −59.3 | −55.2 | −41.7 | −46.6 | 75.2 | |
| $\chi_2^{2,1}$ | | −67.0 | −176.3 | −68.3 | −77.0 | 67.6 | |
| $\chi_2^{2,2}$ | | 169.7 | | 110.2 | 99.5 | −116.9 | |
| $C_{0,1}^{\alpha}-C_0^{\alpha}-C_0'-O_0$ | | −9.5 | 16.1 | 28.5 | 16.0 | 15.7 | |
| $C_{0,2}^{\alpha}-C_0^{\alpha}-C_0'-O_0$ | | 107.7 | 134.6 | 147.4 | 135.0 | 132.7 | |
| $C_{0,3}^{\alpha}-C_0^{\alpha}-C_0'-O_0$ | | −128.6 | −102.9 | −90.2 | −101.3 | −104.2 | |

[a] Angles in degrees. [b] From ref 20. [c] Relative to the atom $C_1^{\gamma}A$ ($C^{\gamma}$-endo form). [d] Relative to the atom $C_1^{\gamma}B$ ($C^{\gamma}$-exo form).

obtained by refinement. Fractional coordinates, equivalent isotropic thermal parameters, anisotropic thermal parameters for the non-hydrogen atoms, calculated fractional coordinates for the hydrogen atoms connected to oxygen or nitrogen atoms, interatomic bond distances, and bond angles have been deposited as supplementary material.

**Infrared Spectroscopy.** Infrared spectra were scanned on a Bruker apparatus IFS 85, working in a Fourier Transform mode. The attention was focused on the most informative frequency domains corresponding to the NH (3200–3500 $cm^{-1}$) and C'O (1600–1750 $cm^{-1}$) stretching vibrations. The concentration was adjusted as to exclude solute–solute interaction, which was verified by further dilution. The solvents used were $CCl_4$ or $C_2Cl_4$ ($5 \times 10^{-4}$ mol $L^{-1}$), $CH_2Cl_2$, MeCN, and $Me_2SO$ ($5 \times 10^{-3}$ mol $L^{-1}$). The spectra were eventually corrected for the residual water contribution by subtraction and cancellation of the OH stretching absorption bands in the 3500–3600 $cm^{-1}$ domain.

**$^1$H NMR Spectroscopy.** Most $^1$H NMR spectra were run in the Fourier Transform mode on a JNM FX 100 spectrometer equipped with a $^{14}$N decoupling unit, giving sharp NH proton signals. Chemical shifts were measured with reference to internal $Me_4Si$. The solvent accessibility of the NH bonds was followed by the solvent perturbation procedure when using a $CHCl_3/Me_2SO$ mixture which proved to be more efficient than the temperature effect for those simple model dipeptides.[25] The vicinal coupling constant $^3J_{N\alpha}$ in the NH–$C^{\alpha}$H system was directly measured on the sharp NH proton signal. The vicinal coupling constants $^3J_{\alpha\beta}$ and $^3J_{\alpha\beta'}$ in the $C^{\alpha}H-C^{\beta}H_2$ systems were calculated on the AB part of the ABX pattern. For complicated spin systems (Xaa = Leu, Met, and Val), $^3J_{\alpha\beta}$ and $^3J_{\alpha\beta'}$ were directly measured on the $C^{\alpha}$H proton signal decoupled from the NH proton transition by using a Brüker AM 400 apparatus.

## X-ray Structures

The precision of the crystal structures depends upon the number of significant reflections measured, the amount of thermal atomic vibrations, and the eventual existence of atomic disorder. In that respect, the crystal structures of L-Pro-L-Tyr and L-Pro-D-Tyr are the most accurate with low thermal parameters even for the *t*-Bu group and the proline cycle (average C–C bond length 1.525 (4) Å and average C–C–C bond angle 103.5 (2)°). Conversely, the atomic disorder of the Pro $C^{\gamma}$ atom and the large thermal coefficients for the *t*-Bu group lead to a much less accurate crystal structure determination for L-Pro-L-Cys(Me).

The geometry of the five dipeptides deserves some comment. The middle and C-terminal amide groups have standard dimensions,[31,32] but sterical hindrances between the bulky *t*-Bu group and the Pro $C^{\delta}$ atom induce some angular variations around C' and N (Figure 1). Another remark concerns the residue Xaa, the average dimensions of which are given in Figure 2. One

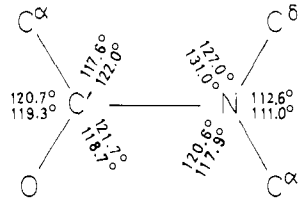


Figure 1. Compared bond angles for the *t*-BuCO-Pro (lower values) and standard X-Pro (upper values, ref 32) amide bonds.

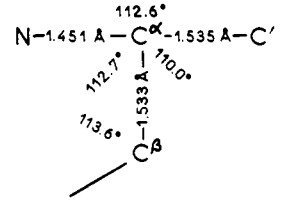


Figure 2. Average bond angles for the Xaa residue.

observes that the N–$C^{\alpha}$–C', N–$C^{\alpha}$–$C^{\beta}$, and $C^{\alpha}$–$C^{\beta}$–$C^{\gamma}$ angles noticeably exceed the standard value 109.5° (the only exception is the $C^{\alpha}$–$C^{\beta}$–$S^{\gamma}$ angle (109.8°) in L-Pro-L-Cys(Me)).

The molecular conformations given in Table II show that all the amide bonds are fairly close to trans planar conformations. The Pro $C^{\gamma}$ atom is out of the plane defined by the other four atoms of the cycle (by approximately 0.5 Å) but the $C^{\gamma}$ puckering is endo in L-Pro-L-Leu, L-Pro-L-Cys(Me) (position A), and L-Pro-L-Phe, and exo in L-Pro-L-Cys(Me)(position B), L-Pro-L-Tyr, and L-Pro-D-Tyr.

All five model dipeptides, exactly as the derivatives *i*-PrCO-L-Pro-L-Ala-NH-*i*-Pr and *i*-PrCO-L-Pro-D-Ala-NH-*i*-Pr already investigated,[20] are folded by a $(i + 3) \rightarrow i$ interaction typical of a $\beta$-turn (Table III). The torsion angles listed in Table II reveal that this turn is of the $\beta$II-type whatever the LL or LD sequence (Figure 3). The only difference between homo- and heterochiral sequences concerns the angle $\Phi_2$ which is systematically smaller in the former case. This probably arises from the close contacts between the Pro oxygen and the Xaa $C^{\beta}H_2$ group (Table IV). One also notes the same orientation of the Xaa side chain, corresponding to the so-called rotamer I of the $C^{\alpha}$–$C^{\beta}$ bond ($\chi^I \simeq -60°$) for an L-residue.

The molecules are arranged in various dispositions in the crystals (Figure 4). However, they are connected by the same $N_2 \cdots O_2$ intermolecular hydrogen bond in all five cases (Table III). Moreover, the oxygen $O_2$ is also strongly bonded to the phenolic hydroxyl group in both L-Pro-L-Tyr and L-Pro-D-Tyr crystals.

(31) Chakrabarti, P.; Dunitz, J. D. *Helv. Chim. Acta* **1982**, *65*, 1555–1562.
(32) Benedetti, E. In "Peptides"; Goodman, M., Meienhofer, J., Eds.; Wiley: New York, 1977; pp 257–273.

Table III. D-H···O[a] Hydrogen Bond Distances (Å) and Angles (deg)

| | data set | D···O | H···O | D-H···O |
|---|---|---|---|---|
| *i*-PrCO-L-Pro-L-Ala-NH-*i*-Pr[b] | | | | |
| $N_3\cdots H_0$[c] | $x,y,z$ | 3.05 | | |
| $N_2\cdots O_2$[d] | $2-x,{}^1/_2+y,1-z$ | 2.79 | | |
| *t*-BuCO-L-Pro-L-Leu-NHMe | | | | |
| $N_3\cdots O_0$[c] | $x,y,z$ | 3.057 | 2.08 | 158 |
| $N_2\cdots O_2$[d] | $1-x,{}^1/_2+y,2-z$ | 2.836 | 1.82 | 168 |
| *t*-BuCO-L-Pro-L-Cys(Me)-NHMe | | | | |
| $N_3\cdots O_0$[c] | $x,y,z$ | 2.935 | 1.91 | 173 |
| $N_2\cdots O_2$[d] | $-x,{}^1/_2+y,1-z$ | 2.746 | 1.82 | 167 |
| *t*-BuCO-L-Pro-L-Phe-NHMe | | | | |
| $N_3\cdots O_0$[c] | $x,y,z$ | 2.999 | 1.98 | 174 |
| $N_2\cdots O_2$[d] | $x,y,z-1$ | 3.010 | 2.07 | 152 |
| *t*-BuCO-L-Pro-L-Tyr-NHMe | | | | |
| $N_3\cdots O_0$[c] | $x,y,z$ | 2.913 | 1.94 | 157 |
| $N_2\cdots O_2$[d] | $x-1,y,z$ | 3.005 | 2.02 | 159 |
| $O_2^{\zeta}\cdots O_2$[d] | $x-1,y-1,z$ | 2.784 | 1.77 | 167 |
| *t*-BuCO-L-Pro-D-Tyr-NHMe | | | | |
| $N_3\cdots O_0$[c] | $x,y,z$ | 2.864 | 1.89 | 158 |
| $N_2\cdots O_2$[d] | $1+x,y,z$ | 3.092 | 2.15 | 151 |
| $O_2^{\zeta}\cdots O_2$[d] | $1-x,{}^1/_2+y,2-z$ | 2.697 | 1.70 | 162 |
| *i*-PrCO-L-Pro-D-Ala-NH-*i*-Pr[b] | | | | |
| $N_3\cdots O_0$[c] | $x,y,z$ | 3.10 | | |
| $N_2\cdots O_2$[d] | $-x,-{}^1/_2+y,2-z$ | 2.91 | | |

[a] The hydrogen atom was moved in the observed D-H direction until the D-H bond length is equal to 1.03 Å. [b] From ref 20; hydrogen atoms not located. [c] Intramolecular 4 → 1 hydrogen bond. [d] Intermolecular hydrogen bond.

Table IV. Short $O_1\cdots C_2^{\beta}$ and $O_1\cdots H(C_2^{\beta})$ Contact Distances (Å)

| | L-Pro-L-Ala | L-Pro-L-Leu | L-Pro-L-Cys(Me) | L-Pro-L-Phe | L-Pro-L-Pro |
|---|---|---|---|---|---|
| $O_1\cdots C_2^{\beta}$ | 3.11 | 3.14 | 3.13 | 3.05 | 3.09 |
| $O_1\cdots H(C_2^{\beta})$[a] | *b* | 2.70 | 2.65 | 2.44 | 2.50 |

[a] Hydrogen atom in the *pro-R* (L-Leu, L-Phe, L-Tyr) or *pro-S* (L-Cys(Me)) position. [b] Hydrogen not located on E-map differences (ref 20).

Table V. NH and CO Stretching Frequencies ($cm^{-1}$) for the *t*-BuCO-L-Pro-Xaa-NHMe Dipeptides in $CH_2Cl_2$[a]

| | | *NH*-Me | | *t*-Bu-*CO* | Pro *CO* | Xaa *CO* |
|---|---|---|---|---|---|---|
| dipeptide | Xaa *NH* | free | bonded | bonded | free | free |
| L-Pro-L-Ala | 3430 | 3450 | 3361 | 1613 | 1681 | 1670 |
| L-Pro-L-Leu | 3430 | 3450 | 3362 | 1613 | 1682 | 1672 |
| L-Pro-L-Val | 3444[b] | 3450[b] | 3362 | 1613 | 1682 | 1670 |
| L-Pro-L-Met | 3425 | 3450 | 3354 | 1611 | 1680 | 1670 |
| L-Pro-L-Cys | 3430[c]/3404 | 3450[c] | 3352 | 1611 | 1682 | 1672 |
| L-Pro-L-Cys(Me) | 3430[c]/3392 | 3450[c] | 3346 | 1609 | 1684 | 1670 |
| L-Pro-L-cys | 3430[c]/3400 | 3450[c] | 3343 | 1609 | 1684 | 1662 |
| L-Pro-L-Cys(S-*t*-Bu) | 3430[c]/3408 | 3450[c] | 3355 | 1611 | 1682 | 1671 |
| L-Pro-L-Phe | 3430[c]/3417 | 3450[c] | 3359 | 1611 | 1682 | 1669 |
| L-Pro-L-Tyr | 3430[c]/3415 | 3450[c] | 3358 | 1612 | 1682 | 1668 |
| L-Pro-D-Ala | 3430 | 3450[c] | 3352 | 1601 | 1689 | 1666 |
| L-Pro-D-Leu | 3428 | 3450[c] | 3352 | 1602 | 1690 | 1667 |
| L-Pro-D-Val | 3435 | 3450[c] | 3352 | 1601 | 1690 | 1666 |
| L-Pro-D-Met | 3423 | 3450[c] | 3348 | 1601 | 1691 | 1666 |
| L-Pro-D-Cys(Me)[d] | 3430[b]/3396 | 3430[b] | 3342 | 1603 | 1691 | 1661 |
| L-Pro-D-Phe | 3423 | 3450[c] | 3348 | 1602 | 1691 | 1666 |
| L-Pro-D-Tyr | 3421 | 3450[c] | 3347 | 1605 | 1690 | 1666 |

[a] Concentration: $5\times10^{-3}$ mol $L^{-1}$. [b] Overlapping absorption bands. [c] Weak shoulder. [d] The NH-*i*-Pr group is substituted for the NHMe group, resulting in lower C-terminal *NH* and Xaa *CO* frequencies by approximately 15 and 5 $cm^{-1}$, respectively (ref 24).

A βII-turn for these five LL-dipeptide sequences seems to be aberrant on the basis of previous results, especially those concerning the L-Pro-L-Leu sequence.[8] It can be argued that intermolecular interactions probably play a more important part for these small molecules, resulting in conformational states which are not found in larger peptides.

### Solute State

The conformational properties of L-Pro-L-Ala and L-Pro-D-Ala have already been reported and interpreted in terms of three rapidly interconverting conformers in $CCl_4$ solution:[24] (i) an open-conformer with free NH and CO bonds; (ii) a γ-folded conformer characterized by a bifurcated $i \leftarrow (i+2) \rightarrow (i+2)$ hydrogen bond; and (iii) a β-folded conformer characterized by a $(i+3) \rightarrow i$ hydrogen bond.

This conformational equilibrium is modified by more polar solvents. Figures 5 and 6 illustrate how γ-folded conformers are converted in weakly acidic chlorinated ($CH_2Cl_2$) or weakly aprotic (MeCN) solvents into the β-folded form which is then converted into the open form in a stronger aprotic solvent ($Me_2SO$).

The strong absorption bands near 3350 and 1600 $cm^{-1}$ ($(i+3) \rightarrow i$ bonded NH(Me) and C′O(*t*-Bu) stretching vibrations, respectively) in the IR spectra of the L-Pro-L-Xaa derivatives in $CH_2Cl_2$ (Table V) reveal that β-folding is the major conformer. We have recently proposed a procedure for the estimation of the β-turn ratio from the shift of the NH(Me) proton NMR signal in $CHCl_3$ and $Me_2SO$ solutions.[25] Results are given in Tables VI and VII. It appears that LL sequences are less β-folded than LD sequences and that the nature of Xaa has a direct influence on their β-folding ratio. The L-Pro-L-Val sequence exhibits the smallest β-folding ratio, and this is probably due to the bulkiness of the Val $C^{\beta}$-branched side substituent. The influence of Xaa supports the existence of some stabilizing interaction between the weakly polar or aromatic side chain and the peptide backbone.

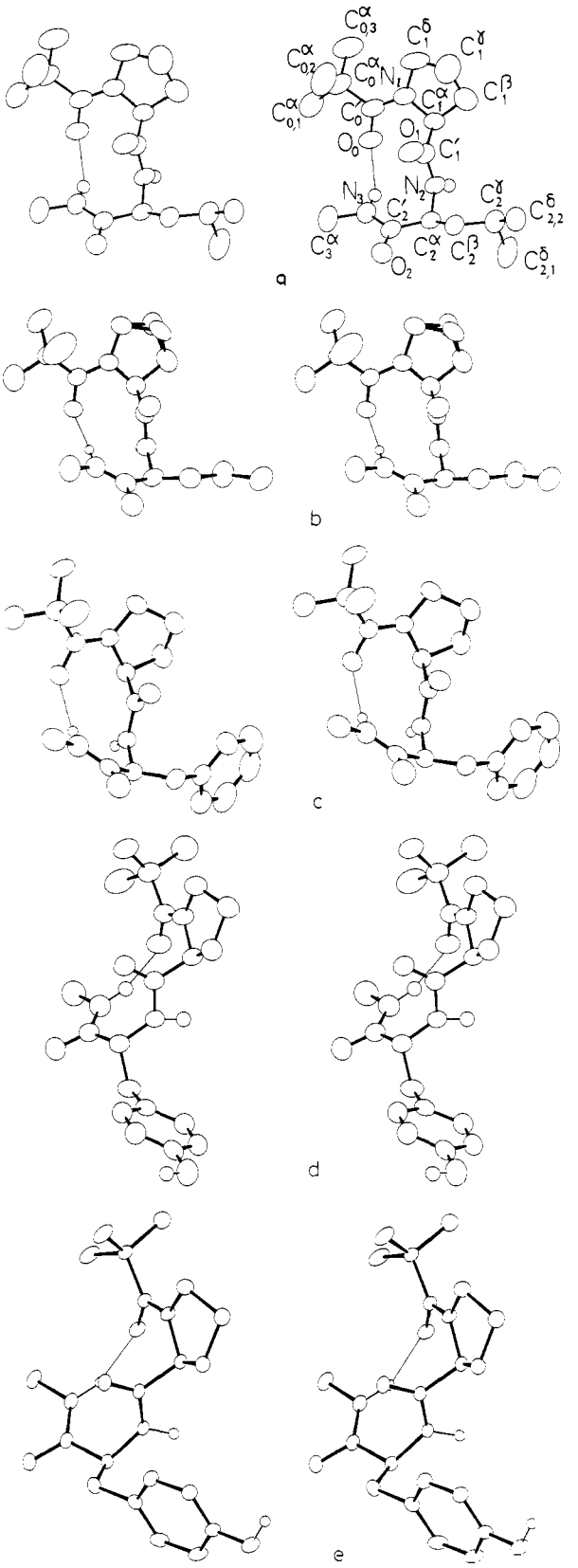


**Figure 3.** Stereoviews of the βII-folded conformation for the L-Pro-L-Leu (a top), L-Pro-L-Cys(Me) (b), L-Pro-L-Phe (c), L-Pro-D-Tyr (d), and L-Pro-L-Tyr (e) derivatives in the crystal. The $(i + 3) \rightarrow i$ hydrogen bond is indicated by the thin line.

IR spectra and $^1H$ NMR data show that the Xaa NH bond is the backbone donor group in this interaction. Its stretching vibration (3430 $cm^{-1}$ in L-Pro-L-Leu ($CH_2Cl_2$), free state) is shifted to lower frequencies by 10 $cm^{-1}$ in L-Pro-L-Phe and by 35 $cm^{-1}$ in L-Pro-L-Cys(Me).

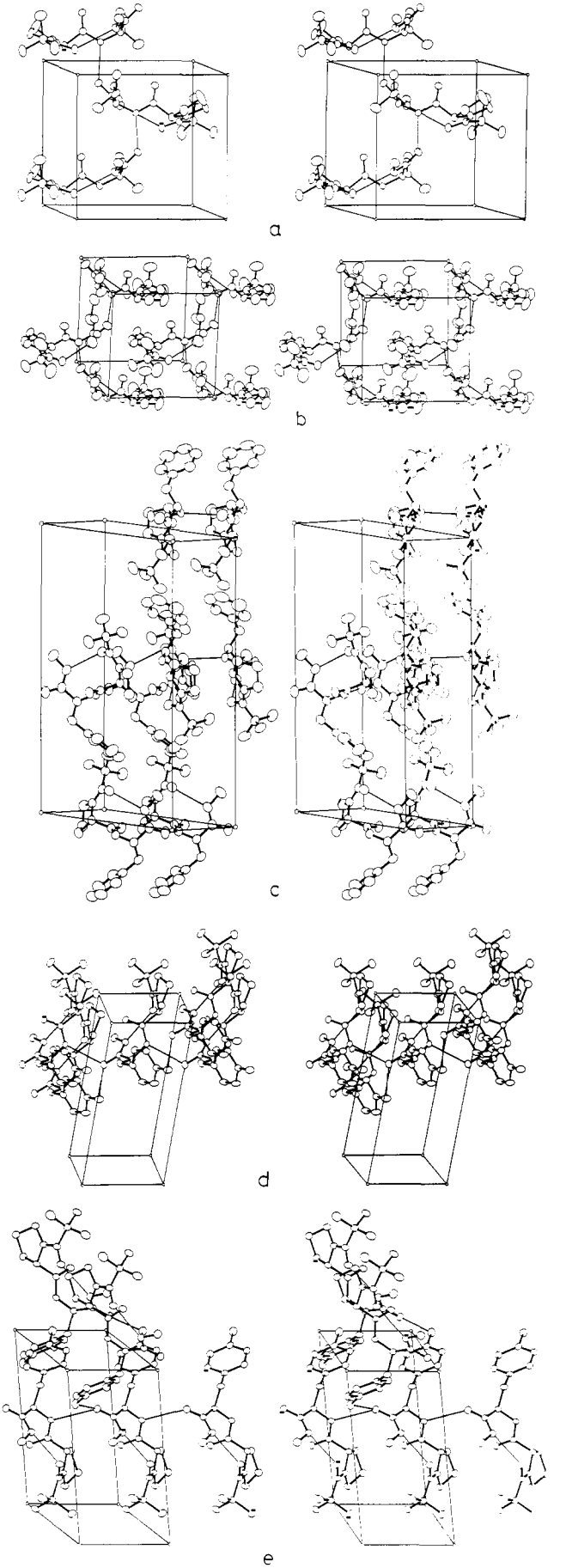


**Figure 4.** Stereoviews of the molecular packing for the L-Pro-L-Leu (a), L-Pro-L-Cys(Me) (b), L-Pro-L-Phe (c), L-Pro-L-Tyr (d), and L-Pro-D-Tyr (e) dipeptides. Hydrogen bonds are indicated by thin lines.

**Table VI.** $^1$H NMR Data for *t*-BuCO-L-Pro-L-Xaa-NHMe in $CHCl_3$[a]

| Xaa | Ala | Leu | Val | Phe | Tyr | Met | Cys | Cys(Me) | cys | Cys(StBu) |
|---|---|---|---|---|---|---|---|---|---|---|
| δNH(Me) | 6.56 | 6.55 | 6.45 | 6.69 | 6.72 | 6.83 | 7.06 | 7.13 | 7.50 | 7.05 |
| δNH(Xaa) | 6.44 | 6.52 | 6.64 | 5.86 | 5.92 | 6.99 | 6.78 | 6.77 | 7.16 | 6.67 |
| $^3J_{N\alpha}$(Xaa) | 8.0 | 8.2 | 9.1 | 9.1 | 9.0 | 8.5 | 8.8 | 8.8 | 9.0 | 8.9 |
| $\Delta\delta$NH(Me)[b] | 1.10 | 1.12 | 1.37 | 0.99 | 0.91 | 0.86 | 0.70 | 0.68 | 0.26 | 0.68 |
| % [β-turn][c] | 57 | 56 | 47 | 62 | 65 | 67 | 73 | 74 | 90 | 74 |
| $\delta H_S^{\beta}$[d] | | *f* | 2.46[h] | 3.43 | 3.33 | *f* | 3.53 | 3.31 | 3.37 | 3.55 |
| $\delta H_R^{\beta}$[d] | | *f* | 2.46[h] | 2.98 | 2.88 | *f* | 2.52 | 2.76 | 2.91 | 2.98 |
| $^3J_{\alpha\beta S}$ | | 10.0[g] | 4.6[h] | 5.6 | 5.1 | 7.3[g] | 3.4 | 4.1 | 6.7 | 5.6 |
| $^3J_{\alpha\beta R}$ | | 4.4[g] | 4.6[h] | 6.2 | 6.2 | 4.8[g] | 4.8 | 5.6 | 4.5 | 4.9 |
| $\lvert^2J_{\beta S\beta R}\rvert$ | | *f* | | 13.8 | 14.0 | *f* | 13.9 | 14.0 | 14.2 | 13.9 |
| % [rot. I][e] | | 8[g] | 10 | 26 | 25 | 12[g] | 12 | 20 | 9 | 13 |
| % [rot. II][e] | | 62[g] | 90[h] | 20 | 15 | 36[g] | 0 | 5 | 31 | 20 |
| % [rot. III][e] | | 30 | 90[h] | 54 | 60 | 52 | 88 | 75 | 60 | 67 |

[a] Chemical shifts δ in ppm, coupling constants *J* in Hz. [b] Variation of the NH(Me) proton signal in $CHCl_3$ and $Me_2SO$. [c] Percentage of β-turn estimated from $\Delta\delta$NH(Me); see ref 24. [d] The *pro-S* and *pro-R* attribution is that for Phe and Tyr and must be inverted for Met and Cys derivatives. [e] Percentages of the Xaa $C^{\alpha}$–$C^{\beta}$ rotamers I, II, and III estimated from ref 48. [f] Not measured. [g] Tentative assignment based on the general predominance of the rotamer II over the rotamer I (ref 56). [h] The Val residue has a single $C^{\beta}H$ proton with a single $^3J_{\alpha\beta}$ coupling constant, giving a global estimation of the rotamers II and III.

**Table VII.** $^1$H NMR Data for *t*-BuCO-D-Pro-L-Xaa-NHMe in $CHCl_3$[a]

| | Ala | Leu | Val | Phe | Tyr | Met | Cys(Me)[i] |
|---|---|---|---|---|---|---|---|
| δNH(Me) | 7.49 | 7.37 | 7.31 | 7.34 | 7.34 | 7.50 | 7.35 |
| δNH(Xaa) | 6.34 | 6.00 | 6.14 | 5.90 | 5.90 | 6.58 | 6.62 |
| $^3J_{N\alpha}$(Xaa) | 8.3 | 9.0 | 9.3 | 9.0 | 9.3 | 8.8 | 8.8 |
| $\Delta\delta$NH(Me)[b] | 0.24 | 0.44 | 0.53 | 0.56 | 0.52 | 0.32 | 0.29 |
| % [β-turn][c] | 91 | 83 | 79 | 78 | 80 | 87 | 89 |
| $\delta H_S^{\beta}$[d] | | *f* | 2.58[h] | 3.29 | 3.25 | *f* | 3.32 |
| $\delta H_R^{\beta}$[d] | | *f* | 2.58[h] | 3.13 | 3.01 | *f* | 2.81 |
| $^3J_{\alpha\beta S}$ | | 10.9[g] | 3.7[h] | 6.3 | 6.4 | 8.3[g] | 4.4 |
| $^3J_{\alpha\beta R}$ | | 3.8[g] | 3.7[h] | 5.7 | 5.6 | 4.1[g] | 5.4 |
| $\lvert^2J_{\beta S\beta R}\rvert$ | | *f* | | 14.0 | 14.4 | *f* | 14.0 |
| % [rot. I][e] | | 2[g] | 2 | 21 | 20 | 5[g] | 18 |
| % [rot. II][e] | | 71[g] | 98[h] | 27 | 28 | 46[g] | 8 |
| % [rot. III][e] | | 27 | 98[h] | 52 | 52 | 49 | 74 |

[a–h] Same as in Table V. [i] Formula *t*-BuCO-D-Pro-L-Cys(Me)-NH-*i*-Pr.

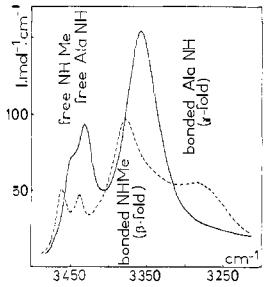


**Figure 5.** NH stretching absorption spectrum for L-Pro-L-Ala in $CH_2Cl_2$ (solid line, $5 \times 10^{-3}$ mol $L^{-1}$) and $CCl_4$ (broken line, $5 \times 10^{-4}$ mol $L^{-1}$). Influence of a weak acidic solvent on the amounts of β- and γ-folded conformers.

This observation is confirmed by the sensitivity of the Xaa NH proton NMR signal to the solvent for $CHCl_3/Me_2SO$ mixtures (Figure 7a). Taking again L-Pro-L-Leu as a standard, the Xaa-NH proton effectively experiences a shielding in L-Pro-L-Phe and a deshielding in L-Pro-L-Cys(Me), both being progressively released by the addition of $Me_2SO$ which has a destabilizing influence on β-turns.

Excepting the L-Pro-D-Cys(Me) dipeptide, these effects are considerably weakened for the heterochiral derivatives (Table V and Figure 7b), suggesting that the Xaa-NH/side chain interaction is less intense in those cases.

The question now arises how to determine the type of β-turns accommodated by the model dipeptides in solution. It has been proposed to discriminate βI- from βII-turns by using the Nuclear Overhauser Effect (NOE) between the $C^{\alpha}H$ of the residue ($i$ + 1) and the NH of the residue ($i$ + 2).[33] Some NOE experiments have been performed on model dipeptides with Xaa = Gly, D-Ala, L-Leu, and L-Val, but the results do not allow a clear-cut conclusion, especially for a probable βI-turn in the L-Pro-LLeu and L-Pro-L-Val sequences.[34] We reached the same conclusion from the NOE coefficients measured on the Pro $C^{\alpha}$ H proton signal

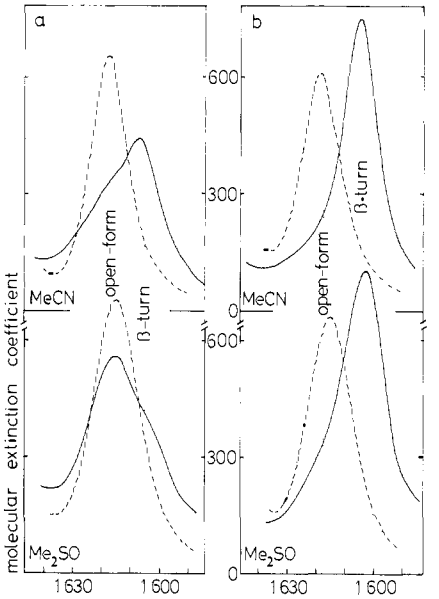


**Figure 6.** CO(*t*-Bu) stretching absorption bands for the homochiral (a) and heterochiral (b) *t*-BuCO-Pro-Ala-NHMe (solid line) and *t*-BuCO-Pro-Me-Ala-OMe (broken line) derivatives in MeCN and $Me_2SO$ ($5 \times 10^{-3}$ mol $L^{-1}$). Influence of a strong aprotic solvent on the amount of β-turn conformation in relation with the chiral sequence.

(33) Khaled, M. A.; Urry, D. W. *Biochem. Biophys. Res. Commun.* **1976**, *70*, 485–491.

(34) Rao, B. N. N.; Kumar, A.; Balaram, H.; Ravi, A.; Balaram, P. *J. Am. Chem. Soc.* **1983**, *105*, 7423–7428. See ref 2 for a discussion of NOE studies on chain reversals in peptides.

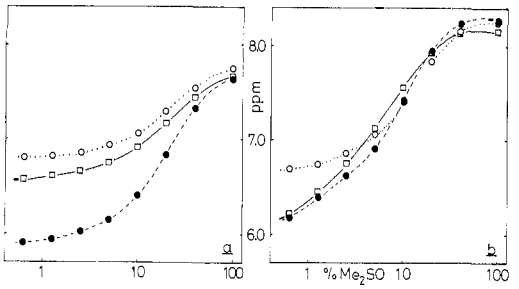


Figure 7. Influence of $Me_2SO$ content on the Xaa NH proton signal for the homochiral (a) and heterochiral (b) Pro-Leu (□), Pro-Phe (●), and Pro-Cys(Me) (○) dipeptides in $CHCl_3/Me_2SO$ mixtures.

for L-Pro-L-Phe and L-Pro-D-Phe (3 ± 2% and 8 ± 2% enhancement, respectively) in a 1:1 mixture of $CHCl_3$ and poly(chlorotrifluoroethylene). We therefore examined the possibilities of other techniques with more reliable correlations: the C'O stretching frequencies and the vicinal coupling constant $^3J_{N\alpha}$ in the NH–C$^\alpha$H fragment.

βI- and βII-turns are mainly differentiated by the rotational states of the C$^\alpha$–C' bond in the residue ($i$ + 1) and of the N–C$^\alpha$ bond in the residue ($i$ + 2).[5]

It has been proved for >CX–C'O– fragments carrying an electronegative substituent X that the C'O stretching frequency is in general split into two components. The higher frequency is assigned to the cis orientation of the polar C—X and C'=O bonds, and the lower one to the trans orientation.[35,36] Similar considerations apply probably also to the C$^\alpha$—N and C'=O bonds in peptides, suggesting that the free C'O stretching frequency in a βII-turn (cis orientation of the C$^\alpha$—N and C=O bonds of the residue ($i$ + 1)) should be higher than in a βI-turn (trans orientation of the same bonds).

The vicinal coupling constant $^3J_{N\alpha}$ should offer another means to discriminate βI- from βII-turns. It is related to the dihedral angle $\theta$ in the NH–C$^\alpha$H fragment ($\theta \simeq 150°$ and 30°, respectively, for a LL sequence). Several forms of $^3J_{N\alpha}(\theta)$ have been proposed,[37,38] but they diverge in the domains of small and large values of $\theta$. However, recent NMR data[39-41] suggest that the correlation of Cung et al.,[37] $^3J_{N\alpha} = 8.6\cos^2\theta - 2.9\cos\theta$ (with $\theta = |\Phi - 60°|$ for an L residue or $\theta = |\Phi + 60°|$ for a D residue), is correctly fitted in those two regions. The distinctive feature of this relation is to assign a high value (11.5 Hz) to $\theta = 180°$, which has now been confirmed by experimental coupling constants exceeding 11 Hz.[39,40] This is also supported by NMR experiments on Boc-L-Cys-L-Pro-Xaa-L-Cys-NHMe peptides (Xaa = L-Ala and D-Ala), with the probable existence of two fused β-turns encompassing the L-Pro-Xaa and Xaa-L-Cys sequences.[41] These β-turns should consequently be of the βI type with $\Phi_{i+2} \simeq 90°$; i.e., $\theta \simeq 150°$ for L-Ala and $\theta \simeq 30°$ for D-Ala. The experimental coupling constants $^3J_{N\alpha}$ are effectively found to be 9.0 ($\theta \simeq 150°$) and 4.5 Hz ($\theta \simeq 25°$). We therefore suggest that βI and βII-turns of an LL sequence should be distinguished by high (9.0 Hz) and low (4.5 Hz) values of $^3J_{N\alpha}$ relative to the residue ($i$ + 2). The opposite should be true for a LD sequence.

Let us return to our model dipeptides. The C'O stretching frequency assigned to the residue ($i$ + 2) is systematically higher by 10 $cm^{-1}$ for the heterochiral sequences (Table V), and both types of sequences are characterized by high $^3J_{N\alpha}$ coupling constants (Tables VI and VII). This is a strong indication of the existence in solution of the classical βI- and βII-folding modes for the LL- and LD-dipeptides, respectively. Small amounts of the other β-folded form cannot be strictly excluded, but the large $^3J_{N\alpha}$ values indicate that its occurrence should be practically negligible in any case.

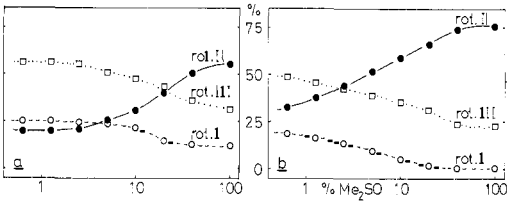


Figure 8. Influence of $Me_2SO$ content on the Xaa C$^\alpha$–C$^\beta$ rotamer distribution for L-Pro-L-Phe (a) and L-Pro-D-Phe (b) in $CHCl_3/Me_2SO$ mixtures.

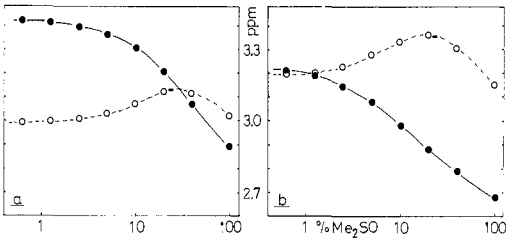


Figure 9. Influence of $Me_2SO$ content on the *pro-S* (●) and *pro-R* (○) L-Phe C$^\beta H_2$ proton signals for L-Pro-L-Phe (a) and D-Pro-L-Phe (b) in $CHCl_3/Me_2SO$ mixtures.

## Discussion

The β-folding mode of the heterochiral dipeptides is found to be invariably of the βII type whatever the solute or crystalline state. The same does not hold true for the homochiral dipeptides which accommodate the βI-folded form in solution and the βII-folded form in the crystal. This shows that the steric hindrances invoked to predict the predominance of the βI-turn[11-18] can easily be circumvented by the molecular packing forces provided there is a slight torsion around the Xaa N–C$^\alpha$ bond. Similar considerations also apply to larger peptides and even more to proteins in which long-range interactions can promote the βII-folding mode of homochiral sequences.[2a,b,3]

The retention of the same intermolecular interaction $N_2\cdots O_2$ in both series of dipeptides in the solid state (Table III) deserves attention. Although the neighboring molecules have different reciprocal dispositions in the seven crystal structures so far resolved, the formation of the $N_2\cdots O_2$ interaction is probably responsible for the βI-to-βII conformational change for the homochiral derivatives. In a βI-turn, the Xaa NH bond is roughly oriented in the same direction as the side chains of both adjacent L-residues, which may prevent a close molecular contact.[42] In a βII-turn, its rotation by nearly 180° makes it more accessible to intermolecular hydrogen bonding which successfully competes with the weak intramolecular interaction involving the Phe, Cys, or Met side chain. Let us mention that a stronger interaction with a polar side chain as in Ser, Thr, or His results in the retention of the βI-turn in the solid state.[43-45]

The existence of this side interaction forces the Xaa C$^\alpha$–C$^\beta$ bond into the so-called rotamer III, $\chi^1 \simeq 60°$, which is generally the less favored disposition.[46,47] The vicinal coupling constants $^3J_{\alpha\beta}$ and $^3J_{\alpha\beta'}$ in the fragment C$^\alpha$H–C$^\beta H_2$ were as usual interpreted in terms of three rapidly interconverting rotamers I ($\chi^1 \simeq -60°$),

(35) Bellamy, S. J. In "Advances in Infrared Group Frequencies"; Methuen: New York, 1968; pp 146–147.
(36) Jones, G. I. L.; Owen, N. L. *J. Mol. Struct.* **1973**, *18*, 1–32.
(37) Cung, M. T.; Marraud, M.; Neel, J. *Macromolecules* **1974**, *7*, 606–613.
(38) Demarco, A.; Llinas, L.; Wuthrich, K. *Biopolymers* **1978**, *17*, 637–650.
(39) Haslinger, E.; Kalchhauser, H.; Wolschann, P. *Monatsh. Chem.* **1984**, *115*, 779–783.
(40) Rich, D. H.; Jasensky, R. D. *J. Am. Chem. Soc.* **1980**, *102*, 1112–1119.
(41) Ravi, A.; Balaram, P. *Tetrahedron* **1984**, *40*, 2577–2583.
(42) Karle, I. L. *J. Am. Chem. Soc.* **1974**, *96*, 4000–4006.
(43) Aubry, A.; Ghermani, N.; Marraud, M. *Int. J. Peptide Protein Res.* **1984**, *23*, 113–122.
(44) Aubry, A.; Marraud, M. *Acta Crystallogr., Sect. C: Cryst. Struct. Commun.* **1985**, *41*, 65–67.
(45) Aubry, A.; Boussard, G.; Marraud, M. In "Peptides, Structure and Function"; Hruby, V. J., Rich, D. H., Eds.; Pierce Chemical Co: Rockford, IL, 1983; pp 817–820.
(46) Janin, J.; Wodak, S.; Levitt, M.; Maigret, B. *J. Mol. Biol.* **1978**, *125*, 357–386.
(47) Benedetti, E.; Morelli, G.; Némethy, G.; Scheraga, H. A. *Int. J. Peptide Protein Res.* **1983**, *22*, 1–15.

II ($\chi^1 \simeq 180°$), and III ($\chi^1 \simeq 60°$) on the basis of a correlation previously established (Tables VI and VII).[48] The amount of rotamer III roughly parallels the βI-turn ratio in $CHCl_3$, and this suggests that the interaction with the side chain has a noticeable stabilizing effect on the βI-turn. This is also supported by the observation that the progressive solvation of the Xaa NH bond by $Me_2SO$ (Figure 7a) is followed by the progressive destabilization of the βI-turn (Figure 6a) together with a decreasing amount of the rotamer III (Figure 8a) and a decreasing magnetic nonequivalence of the $C^\alpha H_2$ protons (Figure 9a).

The high β-turn ratio for heterochiral dipeptides whatever the nature of Xaa (Table VII) suggests that the interaction with the side chain, if any, has a very slight influence on the stability of the βII(LD)-turn conformation. This is confirmed by the retention of the same profile for the *t*-Bu-CO absorption band with increasing $Me_2SO$ content (Figure 6b), whereas the amount of Xaa $C^\alpha$–$C^\beta$ rotamer III noticeably decreases (Figure 8b).

The similar NMR (Table VI) and IR data (Table V) for the four Cys-containing dipeptides deserve to be noted. Whatever the thiol, disulfide, or thioether nature of the sulfur atom, the same N–H···S interaction characterized by the rather low Cys N–H stretching frequency (Table V) is found in solution, resulting in high β-folding ratios (Table VI). The high S–H stretching frequency at 2576 $cm^{-1}$ confirms that the $S^\gamma$–H bond in L-Pro-L-Cys mainly acts as an acceptor site, exactly as the $O^\gamma$–H bond does in the homologous L-Pro-L-Ser derivative.[49,50] A similar N–H···S interaction closing a five-membered cycle has been found in the crystal structure of two cystine derivatives.[51,52]

The assignment of the *pro-S* and *pro-R* protons of the $C^\beta H_2$ group is not straightforward and depends on the solvent (Figure 9). One notes that all dipeptides investigated here and containing a $C^\beta H_2$ group exhibit very similar variations with the solvent composition: one of the $C^\beta H_2$ protons experiences a continuous upfield shift, whereas the other experiences a more complex variation passing through a maximum and crossing the curve relative to the former one. Therefore, the same assignment should probably apply to all cases investigated.

The solvation of the Xaa NH bond leads to an increase of the effective bulkiness of the NH group and in consequence the rotamer II with a trans orientation of the $C^\alpha$–N and $C^\beta$–$C^\gamma$ (or $S^\gamma$) should be favored. Therefore, the $^3J_{\alpha\beta}$ coupling constant increasing with $Me_2SO$ content can be assigned to the *pro-S* or *pro-R* $C^\beta H$ proton according to the L or D configuration of Xaa.[53] In pure $CHCl_3$, the *pro-S* proton of L-Xaa is situated at lower field in accordance with previous observations.[54,55] However, the presence of a crossing point in Figure 9 prohibits a general assignment that would be valid under all experimental conditions.

## Conclusion

Model dipeptides *t*-BuCO-L-Pro-Xaa-NHMe are the smallest molecules capable of β-folding and allowing extensive investigations on the stability of the different β-turn conformations.

The heterochiral dipeptides are generally the more propitious to β-folding, and the β-folding ratio in solution is little dependent on Xaa. The βII-turn is the stable form in both solution and solid state.

The homochiral dipeptides appear to experience much more conformational freedom. In solution, the β-folding ratio depends on Xaa. IR and $^1H$ NMR experiments show that the βI-turn conformation allows an attractive interaction between the Xaa NH bond as the donor group and the polar or aromatic part of the Xaa side chain. This interaction with the side chain contributes greatly to the stability of the βI-turn, and its progressive release by solvation ($Me_2SO$) noticeably decreases the βI-folding ratio. In the solid state, all crystal structures exhibit a βII-turn conformation.

This conformational change (βI-turn → βII-turn) probably arises from the molecular packing forces, which are of particular importance for small dipeptide molecules, and essentially from an intermolecular interaction between the Xaa NH and Xaa C′O groups of two neighboring molecules, exactly as in the crystal structures of the homologous heterochiral derivatives. It indicates that the difference of free energy between the βI- and βII-turn conformations of a homochiral sequence is not so large since it can be compensated for by an intermolecular hydrogen bond.

In larger peptides, long-range interactions can have a similar influence to molecular packing forces in the crystal, and a βII-turn should not be excluded without further investigation. Moreover, a βII(LL)-turn allows closer intermolecular contacts, and this could be of interest for various biological processes involving molecular recognition of peptide molecules.

From an experimental point of view, the βI- and βII-turns can be distinguished by the Pro C′O stretching frequency and the $^3J_{N\alpha}$ coupling constant in the Xaa NH–$C^\alpha$H spin system. The Pro C′O stretching frequency is sensitive to the $C^\alpha$—C′ rotational state: it is higher for the βII-turn (1690 $cm^{-1}$, cis disposition of the Pro N–$C^\alpha$ and C′=O bonds) than for the βI-turn (1680 $cm^{-1}$, trans disposition of the above two bonds). The coupling constant $^3J_{N\alpha}$ is related to the Xaa N–$C^\alpha$ rotational state: a larger value (9 Hz) corresponds to both βI(LL) and βII(LD)-turns (trans orientation of the Xaa N–H and $C^\alpha$–H bonds) and a smaller value (4.5 Hz) to both βI(LD)- and βII(LL)-turns (cis orientation of the above two bonds).

**Acknowledgment.** We thank Prof. Germain for his decisive contribution to solving the L-Pro-L-Tyr crystal structure. We are very grateful to Prof. L. M. Gierasch for fruitful discussions and personal communications prior to publication. We also greatly appreciate the technical assistance of D. Bayeul, J.-M. Grosse, and A. Vicherat.

**Registry No.** *t*-BuCO-L-Pro-L-Ala-NHMe, 53933-24-7; *t*-BuCO-L-Pro-L-Leu-NHMe, 92234-74-7; *t*-BuCO-L-Pro-L-Cys(Me)-NHMe, 98778-87-1; *t*-BuCO-L-Pro-L-Phe-NHMe, 92234-73-6; *t*-BuCO-L-Pro-L-Tyr-NHMe, 98778-88-2; *t*-BuCO-L-Pro-D-Tyr-NHMe, 98778-89-3; *t*-BuCO-L-Pro-D-Ala-NHMe, 53933-27-0; *t*-BuCO-L-Pro-L-Val-NHMe, 92208-85-0; *t*-BuCO-L-Pro-L-Met-NHMe, 98778-90-6; *t*-BuCO-L-Pro-L-Cys-NHMe, 98778-91-7; *t*-BuCO-L-Pro-D-Phe-NHMe, 98778-92-8; *t*-BuCO-L-Pro-L-Cys(*S*-*t*-Bu)-NHMe, 98778-93-9; *t*-BuCO-L-Pro-D-Leu-NHMe, 98778-94-0; *t*-BuCO-L-Pro-D-Val-NHMe, 98778-95-1; *t*-BuCO-L-Pro-D-Met-NHMe, 98778-96-2; *t*-BuCO-L-Pro-D-Cys(Me)-NHMe, 98778-97-3; *t*-BuCO-D-Pro-L-Phe-NHMe, 98778-98-4.

**Supplementary Material Available:** Tables of fractional coordinates, thermal parameters, interatomic bond distances, and bond angles (12 pages). Ordering information is given on any current masthead page.

(48) Cung, M. T.; Marraud, M. *Biopolymers* **1982**, *21*, 953–967.
(49) Aubry, M.; Marraud, M. *Biopolymers* **1983**, *22*, 341–345.
(50) Marraud, M.; Aubry, A. *Int. J. Peptide Protein Res.* **1984**, *23*, 123–133.
(51) Rosenfield, R. E.; Parthasarathy, R. *Acta Crystallogr., Sect. B* **1975**, *31*, 462–468.
(52) Bigoli, F.; Lanfranchi, M.; Leporati, E.; Nardelli, M.; Pellinghelli, M. A. *Acta Crystallogr., Sect. B* **1982**, *38*, 498–502.
(53) The designation *pro-S* or *pro-R* concerns the amino acid residues containing a $C^\gamma$ carbon atom. It must be inverted for the residues containing an $S^\gamma$(Cys) or $S^\delta$ sulfur atom (Met).
(54) Kobayashi, J.; Nagai, U. *Biopolymers* 1978, *17*, 2265–2277.
(55) Tanimura, K.; Kato, T.; Waki, M.; Lee, S.; Kodera, Y.; Izumiya, N. *Bull. Chem. Soc. Jpn.* **1984**, *57*, 2193–2197.
(56) Picur, B.; Slemion, Z. *Org. Magn. Reson.* **1983**, *21*, 271–274.